ANTIOXIDANTS & REDOX SIGNALING
Volume 16, Number 1, 2012

DOI: 10.1089/ars.2011.3898

ORIGINAL RESEARCH COMMUNICATION

Dual Oxidase 2 is Essential for the Toll-Like Receptor 5-Mediated Inflammatory Response in Airway Mucosa

Jung-Hee Joo,[1,2] Ji-Hwan Ryu,[1,2] Chang-Hoon Kim,[1–3] Hyun Jik Kim,[4] Mi-Sun Suh,[5] Jin-Oh Kim,[5] Seung Yeun Chung,[2] Sang Nam Lee,[1,2] Hwan Mook Kim,[5] Yun Soo Bae,[6] and Joo-Heon Yoon[1–3,7]

Abstract

Aims: Airway mucosa is constantly exposed to various airborne microbes, and epithelial host defense requires a robust innate immunity. Recently, it has been suggested that NADPH oxidase (NOX) isozymes serve functional roles in toll-like receptor (TLR)-mediated innate immune responses. However, the molecular mechanism between TLR and NOX-mediated reactive oxygen species (ROS) production in human airway mucosa has been poorly understood. ***Results:*** Here, we show that flagellin-induced ROS generation is dependent on dual oxidase 2 (DUOX2) activation, which is regulated by $[Ca^{2+}]_i$ mobilization in primary normal human nasal epithelial (NHNE) cells. Interestingly, we observed that silencing of DUOX2 expression in NHNE cells and nasal epithelium of *Duox2* knockout mice failed to trigger mucin and MIP-2α production upon challenging flagellin. ***Innovation:*** Our observation in this study reveals that flagellin-induced hydrogen peroxide (H_2O_2) generation is critical for TLR5-dependent innate immune responses, including IL-8 production and MUC5AC expression in the nasal epithelium. Furthermore, DUOX2-mediated H_2O_2 generation activated by the flagellin-TLR5 axis might serve as a novel therapeutic target for infectious inflammation diseases in the airway tract. ***Conclusion:*** Taken together, we propose that DUOX2 plays pivotal roles in TLR5-dependent inflammatory response of nasal airway epithelium. *Antioxid. Redox Signal.* 16, 57–70.

Introduction

The nasal epithelial cells lining the respiratory tract continuously interact with inhaled pathogens, such as viruses and bacteria, leading to dysfunction of the airway epithelium homeostasis (15, 20, 37). Consequently, the airway epithelium provides a physical barrier and secretes signaling molecules against microbial infections (27, 35). Toll-like receptors (TLRs) are indispensable for recognition of pathogen-associated molecular patterns derived from bacteria, viruses, and fungi. TLRs also trigger the activation of innate immune responses (22, 30). Among the ligands of the TLR, flagellin is a common and highly antigenic bacterial antigen present on motile bacteria in mucosa and can bind to TLR5 to stimulate innate immunity (3, 42). In addition, flagellin induces inflammatory cytokine production in various airway epithelial

Innovation

This study provides new insights into understanding of the innate immune and inflammatory response in the airway epithelia. In normal homeostasis with bacteria, hydrogen peroxide (H_2O_2) is continually released to the airway surface liquid to eliminate bacteria, whereas dual oxidase 2 (DUOX2)-mediated H_2O_2 generation regulates host defense by enhancing production of pro-inflammatory mediators (production of IL-8 and MUC5AC) and stimulates adaptive immune responses when the mucosa barrier is irritated by infection. Furthermore, the results from this study may prompt the development of pharmacological inhibitors of DUOX2 as a potential therapeutic approach to control inflammation.

[1]Research Center for Natural Human Defense System, Yonsei University College of Medicine, Seoul, South Korea.
[2]The Airway Mucus Institute, Yonsei University College of Medicine, Seoul, South Korea.
[3]Department of Otorhinolaryngology, Yonsei University College of Medicine, Seoul, South Korea.
[4]Department of Otolaryngology–Head and Neck Surgery, Chung-Ang University College of Medicine, Seoul, South Korea.
[5]Department of Pharmacy, College of Pharmacy, Korea University, Seoul, South Korea.
[6]Department of Life Science, Ewha Womans University, Seoul, South Korea.
[7]BK 21 Project for Medical Science, Yonsei University College of Medicine, Seoul, South Korea.

cells (18, 34, 36). These findings indicate that TLR5 is essential for microbial recognition on the airway mucosal surface.

Substantial evidence has indicated that transient reactive oxygen species (ROS) can be produced by receptor-mediated biochemical processes, although ROS such as superoxide anion and hydrogen peroxide (H_2O_2) have been thought to be by-products of aerobic respiration that could be damaging to DNA, proteins, and lipids. ROS generation for host defense has been extensively studied in terms of NADPH oxidase (NOX) in phagocytic cells. However, after identification of the homologs of gp91phox (NOX1, NOX3-5, and dual oxidase 1-2 [DUOX1-2]) from nonphagocytic cells, the function of the generated ROS has been extended into an understanding of various cellular events, including cell growth, differentiation, apoptosis, and inflammation responses (5, 26). NOX isozymes contain transmembrane domains harboring four heme-binding histidines and conserved NADPH- and FAD-binding sites in a long COOH-terminal region (26). DUOX isozyme contains an additional helix-loop-helix structural domain (EF)-hand that binds Ca^{2+} and extracellular peroxidase-like domain (25, 44). DUOX was originally identified as thyroid oxidase and important in thyroid hormone biosynthesis (5). However, recent studies have focused on a novel function of DUOX isozymes in host–microbe homeostasis for the mucosal

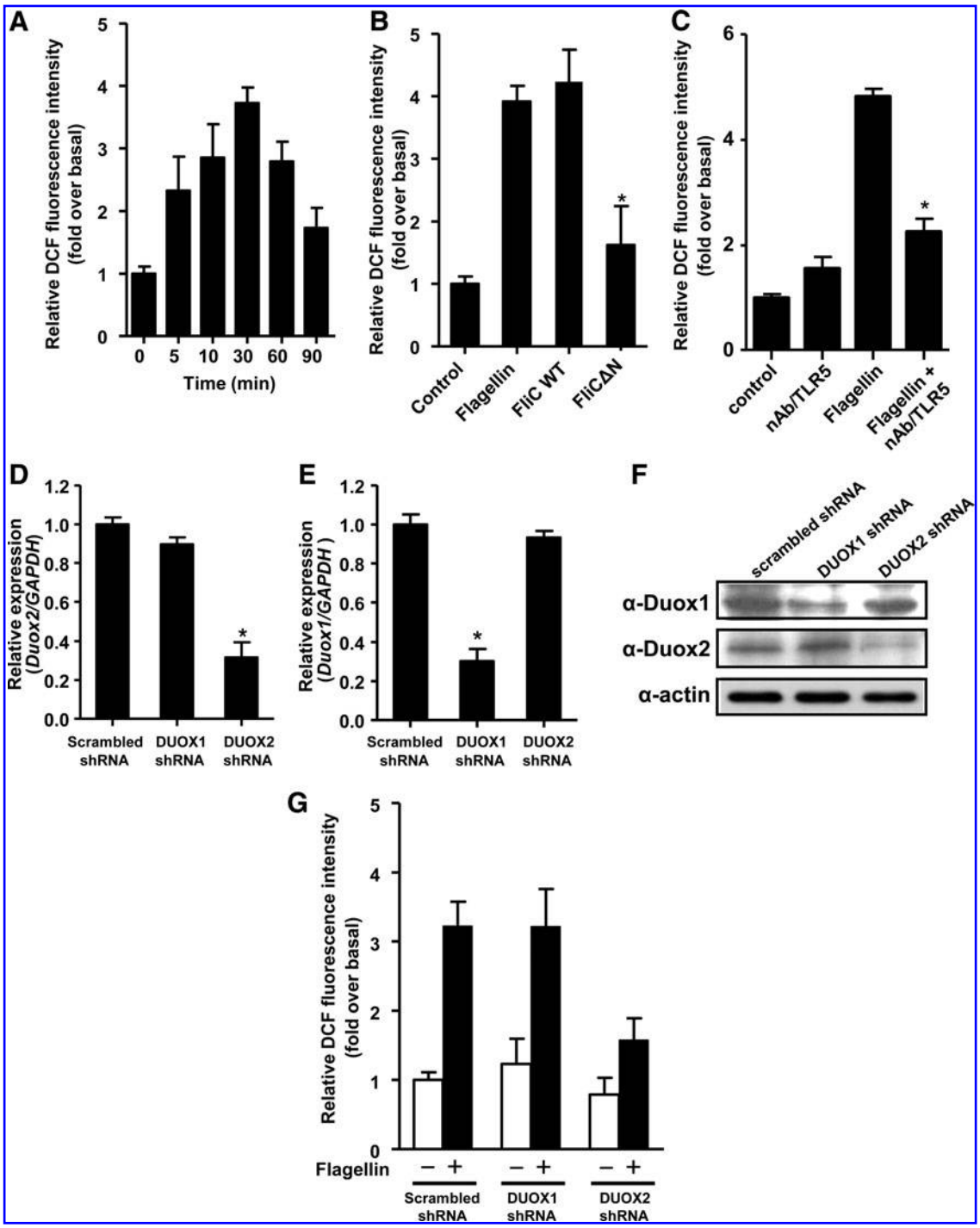

immune response (5, 17). Human DUOX1 and DUOX2 play distinct roles in adaptive immunity of airway epithelial cells, although they have a quite similar structure. Th2 cytokines moderately increase *Duox1* mRNA, whereas Th1 cytokines significantly increase *Duox2* mRNA levels (13).

Recent studies have demonstrated a molecular link between TLR activation and NOX isozymes in innate immune response and host defense, suggesting that NOX activation is indispensable in TLR-mediated innate immune responses (5, 32, 35). We found that flagellin stimulates ROS generation through DUOX2 activation, which is dependent on Ca^{2+} mobilization in primary human nasal epithelial cells. Our results also indicate that flagellin-induced ROS generation through DUOX2 plays a role in TLR5-dependent MUC5AC and IL-8 expression in human airway epithelial cell and mouse mucosa. These results demonstrate that DUOX2-mediated ROS generation is essential for the inflammation process and, therefore, is a novel therapeutic target for infectious inflammatory diseases in the airway.

Results

Flagellin stimulates intracellular ROS production in normal human nasal epithelial cells

The molecular mechanism by which TLR-activated NOX leads to ROS production and triggers inflammation has not been clearly determined (7, 8, 24), although previous reports have reported that Nox is coupled with TLR in inflammation processes. To investigate the function of TLR-induced ROS production in the airway epithelial cells, which play an important role in host defense and inflammation, we stimulated primary normal human nasal epithelial (NHNE) cells with flagellin, a known TLR5 ligand, and then determined intracellular levels of ROS in terms of Nox acitivity by measuring fluorescence of 2′,7′-dichlorofluorescin diacetate (DCF-DA). ROS production increased rapidly within 5 min, reaching its peak at 30 min (3.7-fold over control), and then decreased after 30 min in NHNE cells in response to flagellin stimulation (Fig. 1A). Standard curve with exogenous H_2O_2 (1–1000 μM) in the DCF assay with NHNE cells were prepared and then the level of flagellin-induced H_2O_2 production was analyzed. It is found that the concentration of flagellin-induced H_2O_2 is around 150 μM. FliC, a structure subunit protein that polymerizes to form the filaments of bacterial flagella, is known to activate TLR5 (3, 38). To examine whether the FliC-TLR5 interaction is essential for ROS generation, we purified *Salmonella typhimurium FliC* and the *N*-terminal deleted mutant protein (*FliC*ΔN; 31-118AA), which cannot interact with TLR5 (38). Stimulation of NHNE cells with WT *FliC* protein resulted in increased ROS production (4.2-fold over control), whereas mutant *FliC*ΔN protein failed to induce ROS generation in NHNE cells (Fig. 1B). To confirm the involvement of TLR5 in this process, we explored the effect of neutralizing antibody against TLR5 (nAb/TLR5) on flagellin-induced ROS production in NHNE cells. Pretreatment of NHNE cells with nAb/TLR5 resulted in significantly decreased in ROS generation in response to flagellin (Fig. 1C). These results strongly indicate that interaction of TLR5 with flagellin is required for ROS generation in human airway epithelial cells.

DUOX2 is essential for flagellin-induced ROS generation in airway epithelial cells

We examined the expression level of NOX isozymes in NHNE cells to understand the ROS-generating system of flagellin-stimulated airway mucosa. Quantitative real-time polymerase chain reaction (RT-PCR) indicated that *Duox1* and *Duox2* were the predominant NOX isozymes in NHNE cells. Other NOX isozymes were minor or hardly detectable (Supplementary Fig. S1; Supplementary Data are available online at www.liebertonline.com/ars). The result implies that DUOX isozymes may be responsible for flagellin-induced ROS generation in airway mucosal epithelial cells. Biochemical studies demonstrated that DUOX generates H_2O_2, not superoxide anion (2). Therefore, we note in here that the prominent ROS species in airway mucosal epithelial cells in response to flagellin is H_2O_2.

To explore the roles of DUOX1 and DUOX2 in flagellin-induced H_2O_2 generation, we infected cells with lentiviruses expressing either DUOX1- or DUOX2-targeted shRNA. The infected cells exhibited a marked reduction by 70% in targeted mRNA (Fig. 1D, E). Next, we monitored H_2O_2 production using DCF-DA fluorescence. DUOX2-suppressed cells failed to generate H_2O_2 in response to flagellin, whereas scrambled

FIG. 1. Flagellin stimulates H_2O_2 generation by DUOX2 in NHNE cells. (A) NHNE cells were incubated with flagellin (100 ng/ml) for the indicated times, followed by 10 min incubation with DCF-DA. The generation of intracellular H_2O_2 was monitored by laser-scanning confocal microscopy. Data represent three repeated experiments. The graph of intensity depicts the means ± SD of triplicate cultures. **(B)** NHNE cells were incubated with flagellin (100 ng/ml), *FliC* WT protein (1 μg/ml), and *FliCΔN* lacking of *N* terminal (31-118AA) mutant protein (1 μg/ml). H_2O_2 was monitored by laser-scanning confocal microscopy. *Comparison with *FliC* WT groups, $p < 0.05$. The graph of intensity depicts means ± SD of triplicate cultures. **(C)** Effects of TLR5 antagonist (anti-hTLR5-IgA) on flagellin-induced ROS generation in NHNE cells. Cells were pretreated with TLR5 antagonist (1 μg/ml) for 1 h, and ROS generation was monitored after 10 min of flagellin treatment by laser-scanning confocal microscopy. Data in **C** are mean ± SD ($n = 3$). *Comparison with flagellin-treated control group, $p < 0.05$. **(D–F)** DUOX2 mediates flagellin-induced H_2O_2 generation in NHNE cells. NHNE cells were infected with lentiviruses expressing scrambled shRNA, DUOX1, or DOX2 shRNA, and then allowed to redifferentiate at the air–liquid interface (see the Materials and Methods section for details). **(D)** and **(E)** Compared to scrambled shRNA virus-infected cells, DUOX1 shRNA- or DUOX2 shRNA-transfected cells showed a specific and significant reduction in *Duox1 or Duox2* mRNA relative to *GAPDH* mRNA. *Comparison with scrambled shRNA group, $p < 0.05$. **(F)** Knockdown expression of DUOX1 and DUOX2. NHNE cells were infected with lentivirus expressing scrambled shRNA, DUOX1 shRNA, or DUOX2 shRNA. Cells were subjected into immunoblot analysis with antibodies against DUOX1, or DUOX2. **(G)** H_2O_2 generation in NHNE cells infected with lentivirus containing scrambled shRNA, DUOX1 shRNA, or DUOX2 shRNA was measured by oxidation of DCF-DA under laser-scanning confocal microscopy. Data are presented as mean ± SD ($n = 3$). DCF-DA, 2′,7′-dichlorofluorescin diacetate; DUOX, dual oxidase; H_2O_2, hydrogen peroxide; NHNE, normal human nasal epithelial cells; ROS, reactive oxygen species; SD, standard deviation; TLR, toll-like receptors.

shRNA virus-infected cells exhibited an increase in H_2O_2 (Fig. 1F). Interestingly, DUOX1 shRNA showed no inhibitory effect on H_2O_2 generation in response to flagellin stimulation. These results suggest that DUOX2 is responsible for the majority of flagellin-induced ROS generation in NHNE cells.

Flagellin-induced cytosolic [Ca^{2+}] increase activates DUOX2

Human DUOX enzymes contain canonical calcium-binding EF-hands, suggesting that intracellular calcium ion plays a critical role in activation of DUOX. Furthermore, it has been reported that flagellin induces mobilization of intracellular calcium ion cells *via* ATP production in NCI-H292 cells (28, 29). To investigate flagellin-induced DUOX2 activation mechanism, we analyzed the intracellular calcium concentration ($[Ca^{2+}]_i$) and verified the effect of Ca^{2+} on H_2O_2 production. Stimulation of NHNE cells with flagellin resulted in increases in $[Ca^{2+}]_i$ mobilization (Fig. 2A). Pretreatment of NHNE cells with 1,2-Bis(2-aminophenoxy)ethane-N,N,N′,N′-tetraacetic acid (BAPTA-AM), a Ca^{2+} scavenger, significantly reduced flagellin-induced ROS generation, compared with

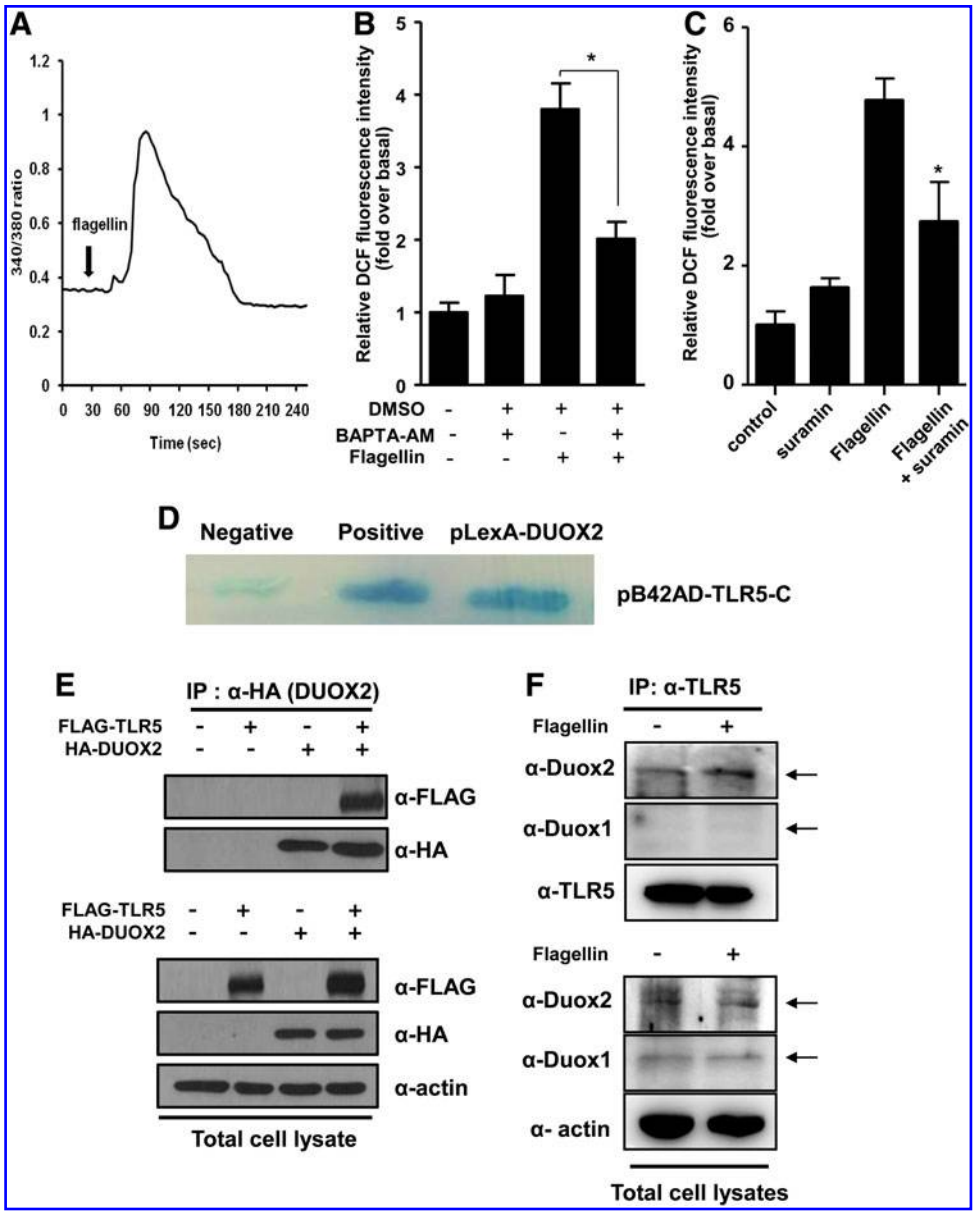

FIG. 2. Flagellin-induced mobilization of cytosolic $[Ca^{2+}]_i$ and interaction of TLR5 with DUOX2. (A) Flagellin-induced calcium influx. Ratiometric Ca^{2+} imaging of NHNE cells loaded with Fura-2/AM shows an increase in the 340/380-nm excitation fluorescence ratio (510 nm emission) after exposure to flagellin at 30 s after detection (*upper panel*). Representative trace is intracellular Ca^{2+} influx in single cells treated with 100 ng/ml flagellin. Experiments were repeated at least five times with similar results. **(B)** Effects of intracellular Ca^{2+} chelating on flagellin-induced ROS generation in NHNE cells. Cells were pretreated with the intracellular Ca^{2+} chelator, BAPTA/AM (10 μM), for 30 min and ROS generation was monitored after 10 min of flagellin treatment by laser-scanning confocal microscopy. Data in **B** are mean ± SD ($n = 3$). *Comparison with flagellin-treated control group, $p < 0.05$. **(C)** Effects of purinergic receptor inhibition on flagellin-induced ROS generation in NHNE cells. Cells were pretreated with inhibitor of nonspecific purigenic receptor, suramin (10 μM), for 30 min, and H_2O_2 generation was monitored after 10 min of flagellin treatment by laser-scanning confocal microscopy. Data in **C** are mean ± SD ($n = 3$). *Comparison with flagellin-treated control group, $p < 0.05$. **(D)** TLR5 interacts with DUOX2. Interactions of TLR5 with DUOX2 were estimated using a yeast two-hybrid assay (see the Methods section). The intensity of *blue* color indicates the expression levels of LacZ and corresponds to the affinity of TLR5 binding with DUOX2. **(E)** pFLAG-CMV-*TLR5* was transiently expresses in HEK293T cells either alone or together with pcDNA3.0-HA-*Duox2*. Cell lysates were then subjected to IP with antibody HA, and the resulting precipitates were subjected to immunoblot analysis with antibodies to FLAG. **(F)** NHNE cell lysates were subjected to IP with antibodies to TLR5. Immunoblot analysis of the resulting precipitates with antibodies to DUOX1 or DUOX2. DMSO, dimethyl sulfoxide; IP, immunoprecipitation; BAPTA/AM, 1,2-Bis(2-aminophenoxy) ethane-N,N,N′,N′-tetraacetic acid. (To see this illustration in color the reader is referred to the web version of this article at www.liebertonline.com/ars).

flagellin-treated control cells (Fig. 2B). This result indicates that flagellin-induced $[Ca^{2+}]_i$ mobilization stimulates DUOX2, resulting in H_2O_2 generation.

Flagellin-TLR5 signaling axis stimulates ATP efflux, leading to activation of purinergic receptor (27, 28). The receptor activates Gαq protein-PLCβ cascade resulting in intracellular calcium mobilization. Suramin is an antagonist of purinergic receptor. We asked whether suramin can prevent H_2O_2 production in response to flagellin. Pretreatment of NHNE with suramin resulted in decreased flagellin-induced H_2O_2 production, suggesting that the activation of purinergic receptor is required for flagellin-dependent H_2O_2 production (Fig. 2C).

Based on the previous reports (7, 33) that a physical interaction between TLR and NOX isozyme plays a critical role in H_2O_2 generation, we performed a yeast two-hybrid assay using the toll/interleukin-1β receptor (TIR) domain of TLR5 as the bait and the COOH-terminal region of the human DUOX2 isozymes (DUOX2-C) as the prey. Yeast cells expressing pB42AD-*TLR5* with pLexA-*Duox2*-C revealed a normal growth and produced blue colonies in the absence of leucine and in the presence of X-gal. The observation indicates that the TIR region of TLR5 interacted with the COOH terminal region of DUOX2 (Fig. 2D). We also performed an immunoprecipitation assay with HEK293 cells co-expressing TLR5 and DUOX2 to confirm the yeast two-hybrid results. The immunoprecipitation complex with antibody to DUOX2 showed an interaction with TLR5 in HEK293 cells (Fig. 2E). To evaluate the interaction of TLR5 with endogenous DUOX2, NHNE cell lysates were subjected to immunoprecipitation with antibodies to TLR5. Immunoblot analysis of the resulting precipitates with antibodies to DUOX2 or DUOX1 revealed that TLR5 interacts with endogenous DUOX2, not DUOX1 (Fig. 2F). However, the interaction was not increased in response to flagellin. These results suggest that DUOX2 localizes with the TLR5 signaling complex and efficiently activates DUOX2 followed by TLR5-induced calcium mobilization.

DUOX2 activation mediates MUC5AC and IL-8 expression induced by flagellin in human airway epithelial cells and the mouse nasal lavage fluid

The inflammatory response is initiated when airway epithelial cells respond to a bacterial or viral infection. Chemokines and inflammation-related molecules, such as IL-8 and MUC5AC, are involved in neutrophil recruitment to the inflamed region in the mucosal epithelium and they provide protection against pathogens (11, 41). We hypothesized that H_2O_2 generation is responsible for inflammatory reactions, such as MUC5AC and IL-8 expression, in response to flagellin stimulation. To elucidate the function of H_2O_2 in inflammation, we analyzed the effect of *N*-acetyl-L-cysteine (NAC) as an ROS scavenger and diphenyleneiodonium sulfate (DPI) as an NOX inhibitor on flagellin-induced MUC5AC and IL-8 expression in NHNE cells. Pretreatment of NHNE with NAC or DPI resulted in a decrease in *MUC5AC* gene expression by 57% and 55%, respectively (Fig. 3A), and a decrease in

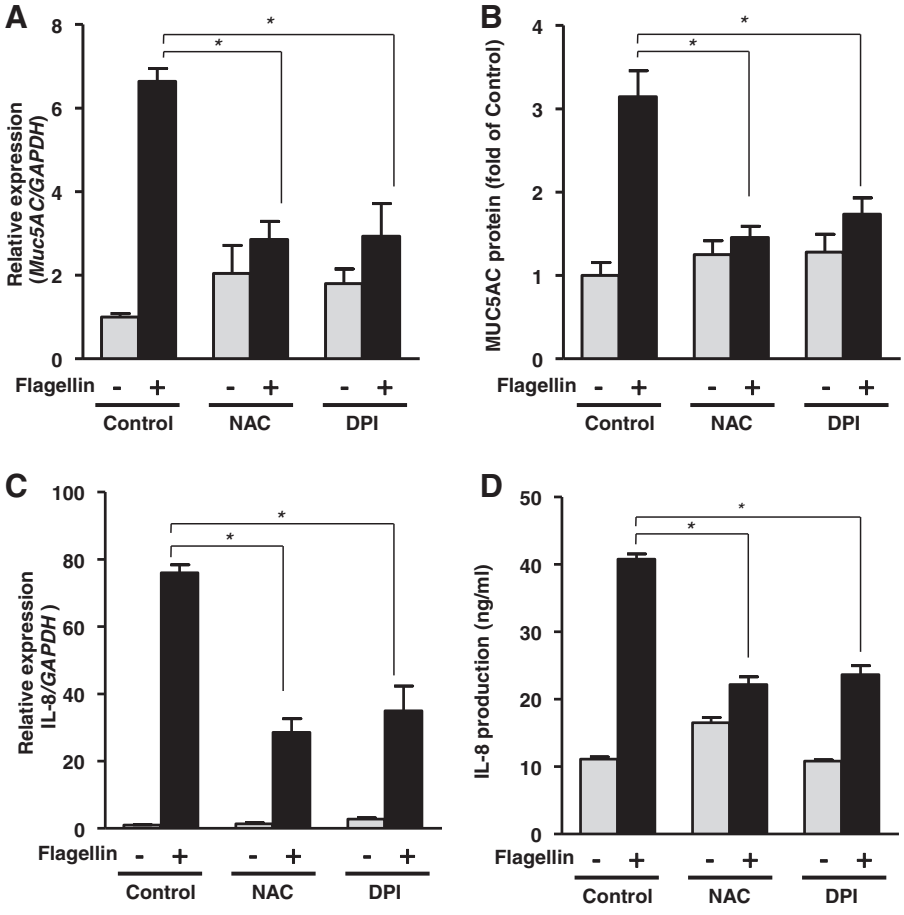

FIG. 3. Inhibition of H_2O_2 generation suppresses flagellin-induced inflammatory response in NHNE cells. (A) and **(C)** NHNE cells were pretreated with NAC (10 μM) or DPI (1 μM) for 30 min and then treated with flagellin for 6 h **(A)** or 1 h **(C)**. After flagellin treatment, *MUC5AC* and *IL-8* mRNA levels relative to *GAPDH* mRNA were measured by RT-PCR. **(B)** and **(D)** NHNE cells were pretreated with NAC (10 μM) or DPI (1 μM) for 30 min and then treated with flagellin for 24 h. After harvesting the upper media, the MUC5AC protein levels were detected by dot blot **(B)** and IL-8 levels were assayed by ELISA **(D)**. Data are presented as the mean ± SD ($n = 3$). *Comparison with flagellin-treated control groups, $p < 0.05$. DPI, diphenyleneiodonium sulfate; ELISA, enzyme-linked immunosorbent assay; NAC, *N*-acetyl-L-cysteine; RT-PCR, real-time polymerase chain reaction.

MUC5AC protein expression by 53% and 45%, respectively (Fig. 3B), in response to flagellin, compared to that of control cells. Moreover, IL-8 (gene expression and protein secretion) were significantly inhibited by the pretreatment of NAC and DPI in NHNE cells (49.4% and 57% to control cells) (Fig. 3C, D). These results suggest that flagellin-induced H_2O_2 generation is indispensable in initiating inflammatory responses, including inflammatory cytokine production and inflammatory-related mucin expression.

To identify the role of DUOX2 in the flagellin-induced inflammatory response in primary human airway epithelial cells, we explored the flagellin-induced inflammatory response in NHNE cells infected with a lentivirus encoding an shRNA specific to DUOX1 and DUOX2. Infection of NHNE cells with a lentivirus encoding a specific shRNA to DUOX1 and DUOX2 resulted in a significant reduction of *Duox1* or *Duox2*, respectively (data not shown). Interestingly, the flagellin-mediated production of MUC5AC and IL-8 (Fig. 4A, B) was significantly reduced in DUOX2 shRNA-transfected cells compared with that in scrambled shRNA-transfected cells. However, knockdown of DUOX1 had no noticeable inhibitory effect on flagellin-induced MUC5AC or IL-8 production (Fig. 4A, B). Thus, these results strongly indicate that DUOX2 has an essential role in flagellin-induced H_2O_2 generation and inflammatory response in NHNE cells.

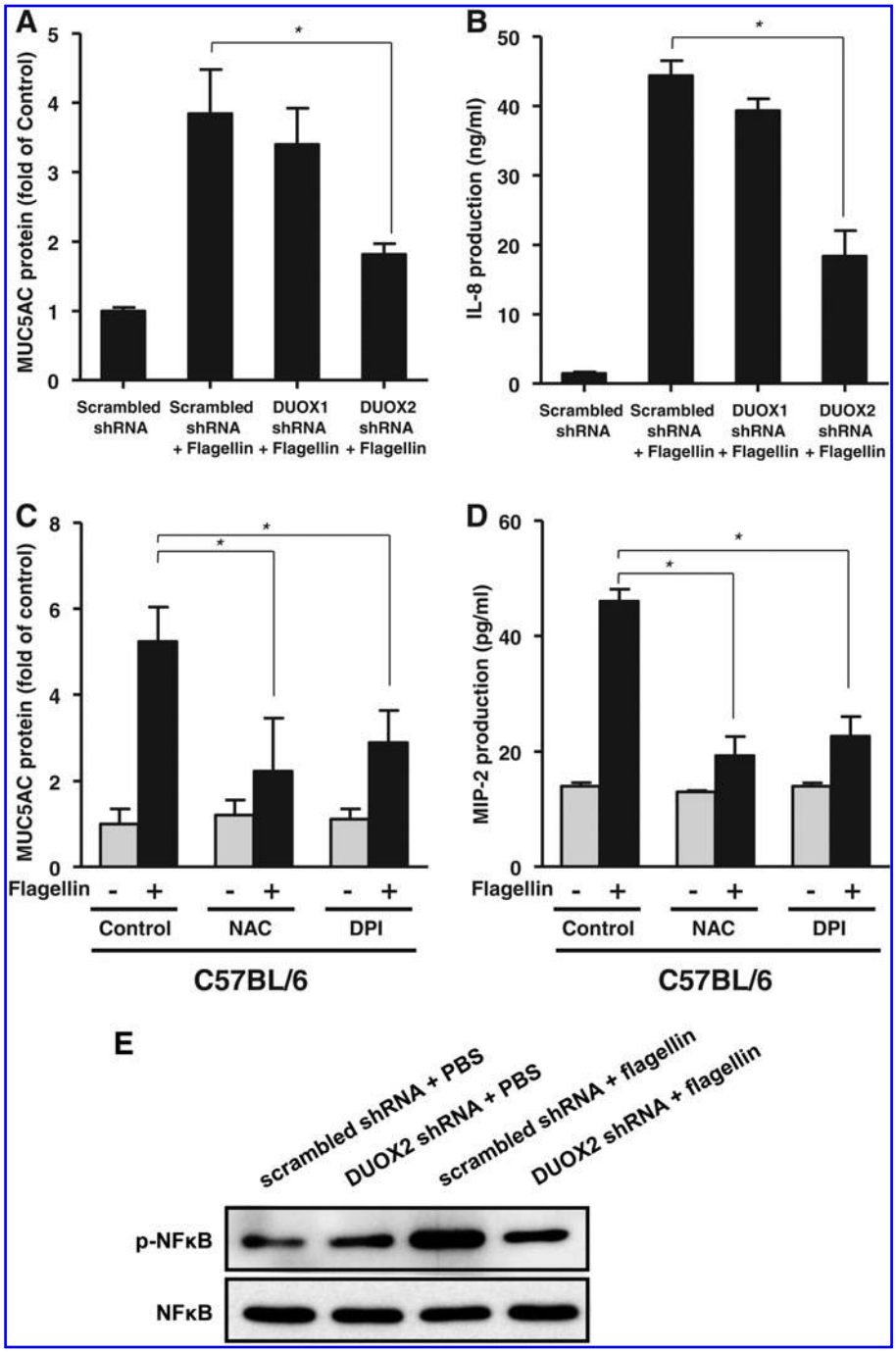

FIG. 4. H_2O_2 generation is essential in the pro-inflammatory response to flagellin. NHNE cells were transfected with either a lentivirus containing DUOX1-specific shRNA, DUOX2-specific shRNA, or scrambled shRNA as described in the Methods section. Cells transfected with a lentivirus containing the scrambled shRNA, or the DUOX1 or DUOX2 shRNA were treated with flagellin for 24 h to measure MUC5AC protein production by dot blot **(A)**. *Comparison with scrambled shRNA group, $p < 0.05$. Cells transfected with a lentivirus containing scrambled shRNA, or DUOX1 or DUOX2 shRNA were treated with flagellin for 24 h to measure IL-8 protein production by ELISA **(B)**. Data are presented as the mean ± SD ($n = 3$). *Comparison with flagellin-treated control groups, $p < 0.05$. **(C, D)** Wild-type mice were pretreated with NAC (100 μM) or DPI (5 μM) for 30 min and administered i.n. without (control) or with flagellin (5 $\mu g/ml$). NALF was collected 12 h after flagellin administration. Then, MUC5AC **(C)** and MIP-2α **(D)** production in NALF were measured by dot blot and ELISA, respectively. Data are representative of two to three independent experiments (nine mice/group). Data are mean ± SD. *Comparison with flagellin treated control groups, $p < 0.05$. Statistical analysis was performed using Student's *t*-test. **(E)** Effect of DUOX2 on NF-κB activation. NHNE cells were infected with lentivirus expressing scrambled shRNA, DUOX1 shRNA, or DUOX2 shRNA. Infected cells were stimulated with flagellin for 15 min and then subjected into immunoblot analysis with antibody against phosphorylated p65 subunit. i.n., intranasal; NALF, nasal lavage fluid; NF-κB, nuclear factor kappa B; PBS, phosphate-buffered saline.

To determine the function of flagellin-induced H_2O_2 generation in the inflammatory response *in vivo*, we examined flagellin-induced MUC5AC and MIP-2α (IL-8 homolog in mouse) in nasal mucosa and nasal lavage fluid (NALF) of C57BL/6 mice in the presence of NAC or DPI. Mice pretreated with NAC or DPI had significantly inhibited the production of MUC5AC (Fig. 4C) and MIP-2α (Fig. 4D) in mouse NALF in response to flagellin compared to mice pretreated with flagellin alone. These results indicate that ROS generation by flagellin might be involved in the acute inflammatory response to bacterial infected *in vivo*. It has been reported that flagellin-TLR5 cascade activates nuclear factor kappa B (NF-κB) leading to immune responses (3). To explore the roles of DUOX2 in flagellin-induced NF-κB activation, NHNE cells were subjected into the knockdown of DUOX2 with lentivirus expressing DUOX2 shRNA. Scrambled shRNA virus-infected cells resulted in increased phosphorylation of p65 subunit, whereas DUOX2-suppressed cells showed a significantly decreased the phosphorylation, indicating that flagellin-mediated DUOX2 activation is essential for the activation of NF-κB (Fig. 4E). These results show that DUOX2 regulates NF-κB activity and production of chemoattractant such as IL-8 and MIP2α.

DUOX2 mutation downregulates the increased inflammation- and immune response- related genes expression induced by flagellin stimulation

We obtained *Duox2* knockout mice from The Jackson Laboratory, which arose by spontaneous C to T transition in exon 16, causing a change from a highly conserved valine^{674} to glycine (21). Next, to evaluate the roles of DUOX2 in flagellin-induced inflammatory response in mouse nasal mucosa, we have performed transcriptional analysis using the Affymetrix GeneChip® Mouse Gene 1.0 ST Array made by Affimetrix, which comprised of more than 770,000 unique 25-mer oligonucleotide features constituting more than 28,000 gene and each gene is represented on the array by 27 probes. The data were processed using the robust multi-array analysis algorithm, which performs a background correction, a normalization step, and a probe-level summary.

Wild type ($Duox2^{+/+}$) and *Duox2* knockout ($Duox2^{-/-}$) mice were stimulated with 1 μg/ml of flagellin for 4 h. Two hundred three genes (greater than twofold) were upregulated in nasal mucosa of $Duox2^{+/+}$ that was treated with flagellin and the full list of genes is presented in Supplementary Table S1. These genes included the following defense-related and immune response-related genes (Table 1 and Fig. 5A): cytokine/chemokine-related genes (*CCL20, CCR2, CCR5, CXCL2, CXCL5, CXCL9, CXCL16, IL18RAP, TNFAIP2, IL1B EAR2*, and *FPR1*), granulocyte-related genes (*IL8RB, MPO, PRG2, PPBP*, and *PRG3*), interferon-related genes (*IFITM6* and *IFI47*), macrophage-related genes (*IL1B* and *S100A9*), and T-cell-mediated immune response-related genes (*H2-Q6* and *IL1F9*). In addition, signal transduction (*PPBP, OLFR60*, and *P2RY10*) and cell adhesion (*SELL, SELP, ICAM1, DSG1A, DSG3*, and *VCAM1*) related genes were also increased by flagellin treatment. These genes were selected based on the biological processes and molecular functions of their gene ontology. However, the increase of inflammation and immune response related genes by flagellin treatment were diminished in the nasal mucosa of the $Duox2^{-/-}$ mice compared with that of $Duox2^{+/+}$ mice (Table 1 and Fig. 5A).

To confirm the microarray result, we measured flagellin-induced MUC5AC and MIP-2α (CXCL2) production in *Duox2* knockout ($Duox2^{-/-}$) mice compared with that in $Duox2^{+/+}$ and $Duox2^{+/-}$ mice. Although MUC5AC was not selected by twofold increased gene, flagellin-induced production of MUC5AC (Fig. 5B) and MIP-2α (Fig. 5C) were diminished in the nasal mucosa of the $Duox2^{-/-}$ mice compared with that of $Duox2^{+/+}$ and $Duox2^{+/-}$ mice. However, the change in flagellin-induced MUC5AC and MIP-2α production was insignificant in heterozygous $Duox2^{+/-}$ mice and in $Duox2^{+/+}$ mice.

Neutrophil infiltration and MUC5AC expression were reduced in the nasal epithelium and NALF of $Duox2^{-/-}$ mice

Increasing of neutrophil infiltration is hall mark in inflamed tissue. We performed histological analysis of neutrophil infiltration in nasal epithelium of $Duox2^{-/-}$, $Duox2^{+/-}$, and $Duox2^{+/+}$ mouse. Mouse nasal epithelium was injected by challenging of flagellin and then subjected into immunohistochemical staining with antibodies to neutrophil and MUC5AC protein in mouse nasal mucosal epithelium. Neutrophil infiltration was significantly decreased in the nasal epithelium of $Duox2^{-/-}$ mice and NALF of $Duox2^{-/-}$ mice compared to $Duox2^{+/-}$ and $Duox2^{+/+}$ (Fig. 6A, B). Moreover, MUC5AC expression was abolished on the surface of the nasal mucosa of $Duox2^{-/-}$ mice compared to $Duox2^{+/-}$ and $Duox2^{+/+}$ (Fig. 6C). Taken together, these results suggest that DUOX2 activation is essential for TLR5-induced inflammatory responses in nasal mucosal epithelium.

DUOX2 expression is upregulated in nasal mucosa of acute sinusitis

Consistent with critical role of DUOX2 in inflammation, we explored the level of *Duox2* expression in nasal inflammatory biopsies of patients suffering from infectious sinusitis (nonallergic) in comparison to non-inflammatory tissue in nasal mucosa of healthy volunteers. Nasal mucosa from 11 adult patients with nonallergic sinusitis and 11 nonallergic normal adults were subjected into RT-PCR measuring the expression levels of *Duox2* (Fig. 7A). Interestingly, we found a significant increase in the *Duox2* gene expression level in sinusitis, compared to that in healthy adults. Moreover, neutrophil infiltration was increased in sinusitis (Fig. 7B). In conclusion, the upregulated expression of *Duox2* seems to be linked to infectious inflammatory diseases in the nasal mucosa.

Discussion

The DUOXs so far are mainly known to be responsible for H_2O_2 generation, as seen in thyrocytes where they catalyze iodination of thyrogloubulin by stimulating thyroperoxidase (31). In addition to DUOX expression in the thyroid, DUOX1/2 isozymes are expressed in the ducts of the salivary gland, airway epithelia, and intestinal colon epithelium. Because DUOX has a peroxidase-like ectodomain in the NH3-terminal region, DUOX can directly generate H_2O_2 (10, 12). Substantial evidence indicates that both DUOX-dependent H_2O_2 and lactoperoxidase generate hypothiocyanate ($OSCN^-$) from the oxidation of SCN^-, providing a robust antimicrobial defense network in epithelial cells.

Table 1. Gene Analysis and Quantification of Inflammatory Molecules in Flagellin-Treated Nasal Mucosa of Mice

TargetID	mRNA accession	Gene symbol	Fold change: Duox2$^{+/+}$-F[a]/ Duox2$^{+/+}$-C[b]	Duox2$^{-/-}$-C[c]/ Duox2$^{+/+}$-C	Duox2$^{-/-}$-F[d]/ Duox2$^{-/-}$-C	Duox2$^{-/-}$-F/ Duox2$^{+/+}$-F
A. Immunity and Defense						
10589535	NM_008694	NGP	7.83	1.21	−1.12	−2.73
10473399	NM_008920	PRG2	5.75	2.18	1.41	−1.87
10347888	NM_016960	CCL20	5.56	1.36	1.87	−2.19
10523156	NM_009140	CXCL2	5.39	1.18	2.40	−1.90
10523128	NM_023785	PPBP	3.91	−1.42	1.53	−3.63
10398665	NM_009396	TNFAIP2	3.90	−1.33	1.84	−2.82
10493831	NM_013650	S100A8	3.56	1.74	1.37	−1.50
10481627	NM_008491	LCN2	3.31	−1.52	2.49	−2.01
10570610	NM_019728	DEFB4	3.20	−1.01	−1.55	−5.02
10414262	NM_007895	EAR2	3.15	1.24	−1.18	−3.01
10569020	NM_001033632	IFITM6	3.08	1.33	1.18	−1.97
10469786	NM_153511	IL1F9	2.89	−1.49	1.23	−3.50
10444824	NM_207648	H2-Q6	2.67	−1.21	−1.10	−3.56
10496592	NM_010260	GBP2	2.54	−2.01	1.11	−4.61
10493834	NM_207263	PGLYRP4	2.51	−1.05	−1.06	−2.80
10487597	NM_008361	IL1B	2.46	−1.31	2.13	−1.50
10347291	NM_009909	IL8RB	2.38	1.39	1.23	−1.40
10590631	NM_009915	CCR2	2.37	−1.09	−1.55	−4.00
10448124	NM_013521	FPR1	2.33	1.31	1.18	−1.51
10541614	NM_010819	CLEC4D	2.31	1.37	1.20	−1.40
10499861	NM_009114	S100A9	2.22	1.23	1.29	−1.40
10380174	NM_010824	MPO	2.20	1.04	1.26	−1.67
10531407	NM_008599	CXCL9	2.15	1.15	1.27	−1.48
10547664	NM_019948	CLEC4E	2.13	1.49	1.24	−1.15
10496539	NM_153564	GBP5	2.13	−1.47	1.53	−2.05
10345824	NM_010553	IL18RAP	2.08	1.08	1.40	−1.38
10375515	NM_008330	IFI47	2.05	−1.16	−1.00	−2.38
10583519	NM_010493	ICAM1	2.01	−1.05	1.66	−1.26
10387890	NM_023158	CXCL16	2.00	−1.32	1.08	−2.45
B. Signal Transduction						
10523128	NM_023785	PPBP	3.91	−1.42	1.53	−3.63
10568956	NM_146955	OLFR60	3.00	1.23	2.12	−1.15
10469786	NM_153511	IL1F9	2.89	−1.49	1.23	−3.50
10487597	NM_008361	IL1B	2.46	−1.31	2.13	−1.50
10347291	NM_009909	IL8RB	2.38	1.39	1.23	−1.40
10541061	NM_146912	OLFR211	2.22	1.39	1.59	−1.00
10601416	NM_172435	P2RY10	2.15	−1.00	−1.02	−2.18
C. Cell Adhesion						
10351197	NM_011346	SELL	2.65	1.38	1.27	−1.51
10351206	NM_011347	SELP	2.15	−1.17	1.07	−2.36
10454113	NM_010079	DSG1A	2.13	1.09	−1.15	−2.24
10454154	NM_030596	DSG3	2.12	−1.75	−1.18	−4.39
10439744	NM_032465	CD96	2.09	1.18	1.23	−1.44
10501608	NM_011693	VCAM1	2.06	1.24	−1.06	−1.77
10583519	NM_010493	ICAM1	2.01	−1.05	1.66	−1.26

[a]Flagellin-treated nasal mucosa of wild-type mice (C57BL/6).
[b]PBS-treated nasal mucosa of wild-type mice (C57BL/6).
[c]PBS-treated nasal mucosa of *Duox2* knockout (*Duox2*$^{-/-}$) mice.
[d]Flagellin-treated nasal mucosa of *Duox2* knockout (*Duox2*$^{-/-}$) mice.

Although excess production of H_2O_2 by chronic infection and pathophysiological stress is detrimental to tissues, several recent reports have indicated that H_2O_2 is widely present as a key regulator in intracellular signaling related to immunity and inflammation (41, 43, 45). In this study, we first found that DUOX2-induced H_2O_2 is essential for the TLR5-dependent inflammatory response in primary NHNE cells and murine nasal mucosa; we tested DUOX1-knockdown NHNE cells and found no inhibitory effect on flagellin-induced H_2O_2 generation. However, when we silenced DUOX2 in the cells, H_2O_2 generation was inhibited in response to flagellin (Fig. 1F). Earlier studies have reported that DUOX1 is the major source of H_2O_2 in TLR-mediated cell signaling in the epithelial cells of the lower respiratory tract (9, 24, 41, 45). However, in

NHNE cells, our results suggest that DUOX2 controls the flagellin-induced ROS generation and hence is involved in the inflammatory response. The discrepancy between those results and ours can be explained by a difference in experimental conditions. First, unlike the previous reports that used epithelial cells of the lower respiratory tract, we examined the flagellin-induced response in primary NHNE cells. Second, we focused on TLR5-mediated inflammatory responses induced by flagellin, whereas previous reports analyzed asialoGM1 function in epithelium (9, 45). The activating antibody against asialoGM1 (α-ASGM1) ligates the asialoGM1 receptor, not TLR5 (1). Our finding of the DUOX2 activation mechanism by flagellin stimulation is quite consistent with the recent researches for DUOX2-induced host defense mechanism in *Drosophila* gut immunity (17) and *Helicobacter pylori*–induced chronic inflammation of the gastric cavity (19). Third, DUOX1 and DUOX2 activities are mainly regulated by mobilization of intracellular calcium. However, additional mechanisms regulating their intrinsic activity are different; DUOX1 is positively regulated by the cAMP-dependent protein kinase A (PKA) cascade, whereas DUOX2 is highly induced by activation of PKC stimulated by PMA (39). It is well known that purinergic receptor stimulates PLCβ, leading to IP3 production for intracellular calcium mobilization and DAG generation for activation of PKC. Flagellin-TLR5 cascade may induce PLCβ-PKC pathway resulting in specifically DUOX2 activation in nasal epithelium. These recent results suggest that DUOX2 plays an important role in mucosal immunity in a wide range of species, from flies to humans.

Considering our data in conjunction with a previous study (14), we can hypothesize that a rapid and transient (5–10 min) increase in intracellular H_2O_2 may act as intracellular second messenger in TLR5-induced cell signaling, whereas an increase in H_2O_2, a result of a prolonged response to flagellin (>6 h), kills invasive microorganisms as part of the host defense mechanism. We also found that *Duox2* expression was increased after 6-h treatment with flagellin (data not shown). However, increasing *Duox2* expression could not explain the early and transient increase in H_2O_2 in response to flagellin stimulation. This disparity in ROS generation and *Duox2* expression may indicate the existence of rapid and efficient regulation of DUOX2 activation. Several lines of evidence indicated that TLR5 induces intracellular calcium ($[Ca^{2+}]_i$) mobilization through ATP production as a purinergic agonist (9, 28). This observation explained why activation of DUOX containing EF hands can be regulated by ATP-dependent

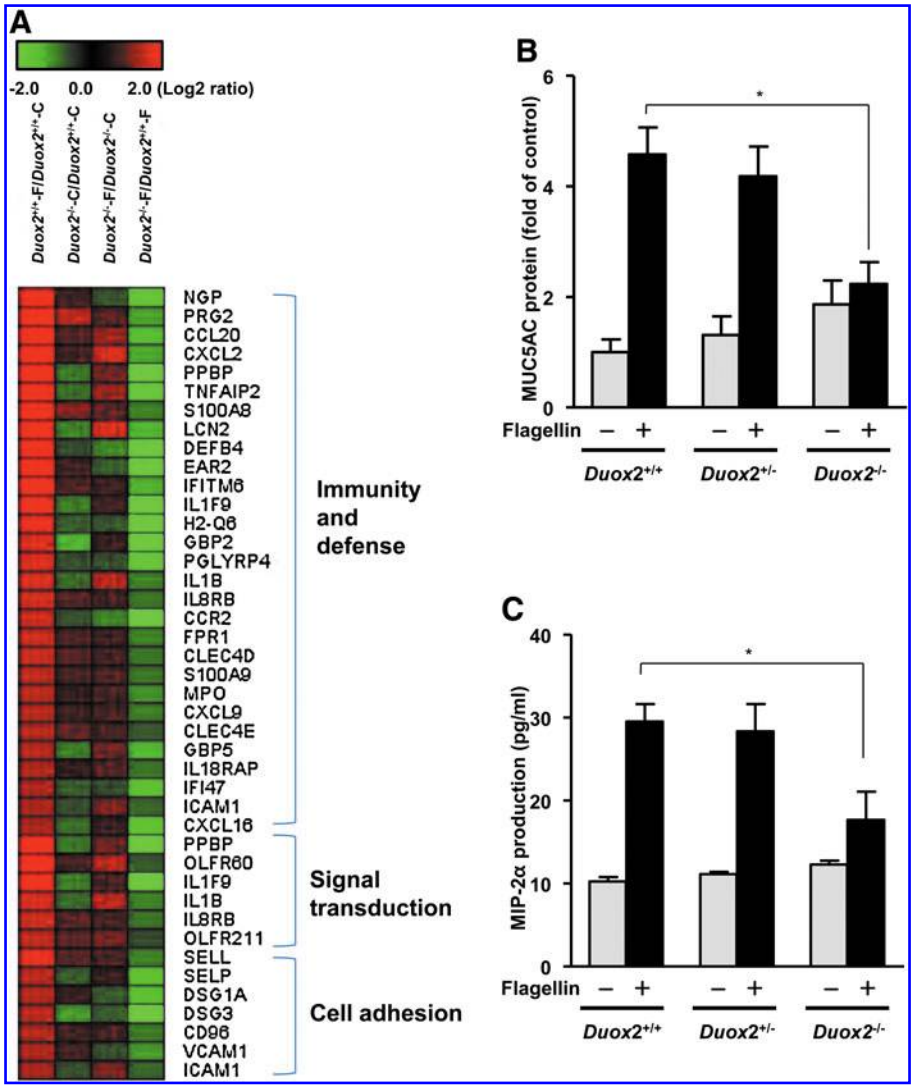

FIG. 5. Gene analysis and quantification of inflammatory molecules in flagellin-treated nasal mucosa of *Duox2*$^{-/-}$ mice. (A) The indicated mice received either PBS (control) or flagellin (5 μg/ml) intranasally for 4 h. Data were presented as a matrix; each row represents an individual array element (gene), and each column represents an experimental condition. Data were expression profiles of immunity and defense, signal transduction, and cell adhesion-related genes differentially regulated by flagellin with greater than or equal to twofold induction. *Red* represented relative upregulation, whereas *green* represented downregulation (see scale, *upper bar*). **(B, C)** NALF was collected 12 h after flagellin administration and MUC5AC **(B)** and MIP-2α **(C)** production in NALF were measured by dot blot and ELISA, respectively. Data are representative of three independent experiments (nine mice/group). Data in **(B, C)** are presented as the mean ± SD. *Comparison with flagellin-treated WT groups, $p < 0.05$. (To see this illustration in color the reader is referred to the web version of this article at www.liebertonline.com/ars).

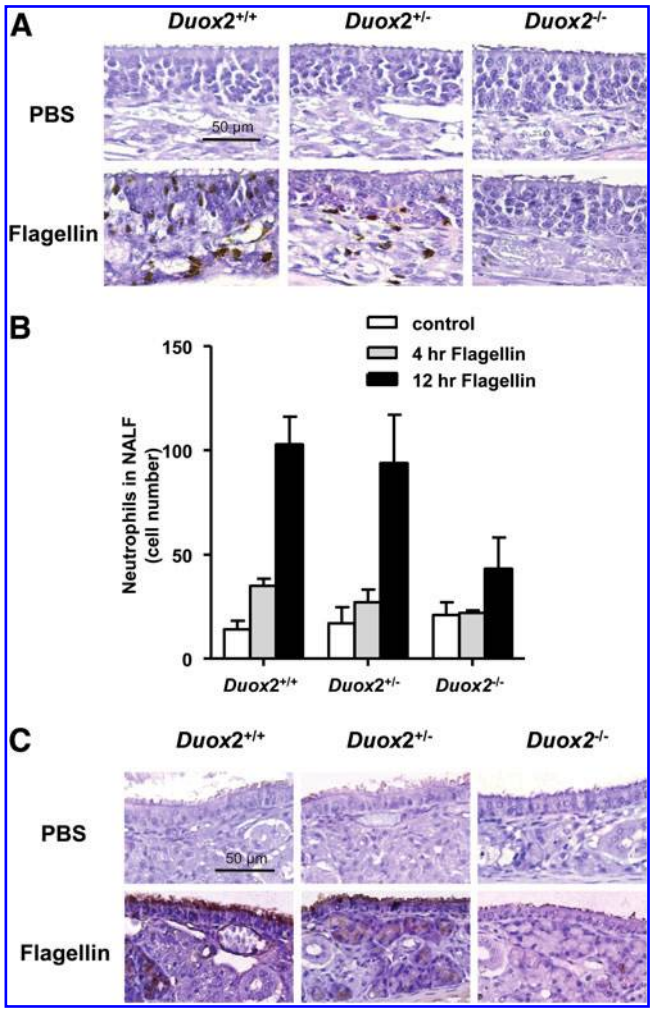

FIG. 6. Flagellin failed to trigger an inflammatory response in the upper airway of *Duox2*$^{-/-}$ mice. (A) Neutrophil infiltrating in the nasal mucosa of mice 12 h following i.n. instillation of flagellin or control (PBS). Immunohistochemical staining of neutrophils in nasal mucosa of WT and *Duox2* mutant mice after i.n. instillation of flagellin or the control (PBS) for 12 h. Three independent experiments were obtained from similar results. **(B)** NALF was collected after 4 or 12 h after flagellin administration and infiltrated neutrophils in NALF were counted (See Methods section). Data in **(B)** are presented as the mean ± SD and representative of three independent experiments (nine mice/group). **(C)** Immunohistochemical expression of MUC5AC from WT and *Duox2*-mutant mice following i.n. instillation of flagellin or the control (PBS) for 12 h. Three independent experiments were obtained from similar results. (To see this illustration in color the reader is referred to the web version of this article at www.liebertonline.com/ars).

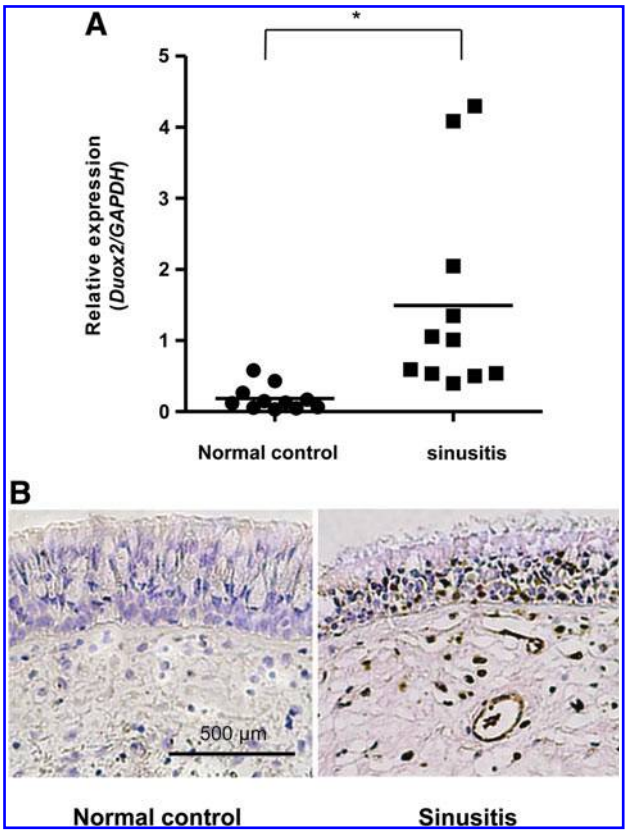

FIG. 7. Duox2 expression is upregulated in nasal mucosa of acute sinusitis. (A) Expression of Duox2 in nasal tissues in sinusitis patients. Total RNA was isolated from nasal biopsies of patients with nonallergic sinusitis (Sinusitis; $n = 11$) or nonallergic healthy controls (Normal control; $n = 11$ each). RT-PCR was performed for DUOX2 and GAPDH, and relative expression of DUOX2 was compared with control (GAPDH). Data are mean ± SD ($n = 11$). *Comparison with normal control groups, $p < 0.05$. Statistical analysis was performed using Student's *t*-test. **(B)** Neutrophil infiltrating in nasal tissues in sinusitis patients. Immunohistochemical staining of neutrophils in nasal tissues of patients with nonallergic sinusitis (Sinusitis) or nonallergic healthy controls (Normal control). Three independent experiments were obtained from similar results. (To see this illustration in color the reader is referred to the web version of this article at www.liebertonline.com/ars).

$[Ca^{2+}]_i$ mobilization. These studies showed that H_2O_2 production in flagellin-stimulated cells is mediated by the sequential activation of TLR5, ATP release, activation of purinergic receptor, and an increase in intracellular calcium, which then binds to the EF hand of DUOX to stimulate its oxidase activity. Here we found that flagellin-stimulated $[Ca^{2+}]_i$ mobilization and scavenging of $[Ca^{2+}]_i$ in response to the addition of BAPTA and EGTA/thapsigargin suppresses flagellin-mediated H_2O_2 generation (Fig. 2, Supplementary Fig. S2). Yeast two-hybrid and immunoprecipitation analysis revealed that the COOH-terminal region of DUOX2 interacts with the COOH-terminal region of TLR5 (Fig. 2D–F). Moreover, immunoprecipitation analysis showed that an endogenous DUOX2 interacts with TLR5 (Fig. 2F). It is evident that DUOX2 and TLR5 constitute a multi-protein complex in a signaling cascade. Based on this observation, we propose that $[Ca^{2+}]_i$ mobilization and DUOX2 localization in the TLR5 signaling complex serves proper activation of DUOX2 in response to flagellin stimulation.

In this study, we also evaluated expression of MUC5AC, an inflammation-related mucin and secretion of IL-8 as neutrophil attractant in flagellin-induced inflammatory responses to understand the roles of DUOX2-mediated ROS generation in NHNE cells. Pretreatment of NAC (an ROS scavenger), diphenyliodonium (a NOX inhibitor), or transfection of DUOX2-specific shRNA into NHNE cells resulted in inhibited

expression of MUC5AC and secretion of IL-8 (MIP-2α in mice) in response to flagellin stimulation (Figs. 3–5). We confirmed that flagellin failed to trigger an inflammatory response (MUC5AC expression and neutrophil infiltration) in the nasal mucosa of *Duox2*$^{-/-}$ mice compared to that of wild-type and *Duox2*$^{+/-}$ mice (Fig. 6). Interestingly, microarray results showed that many genes related to neutrophils were reduced in *Duox2*$^{-/-}$ mice (Fig. 5). These results indicate that expression of inflammatory molecules was inhibited in *Duox2* mutant mice resulting in the reduction of neutrophil infiltration.

Consistent with critical role of DUOX2 in inflammation, we explored the level of *Duox2* expression in nasal inflammatory biopsies of patients suffering from infectious sinusitis (nonallergic) in comparison to noninflammatory tissue in nasal mucosa of healthy volunteers. Nasal mucosa from 11 adult patients with nonallergic sinusitis and 11 noninflamed normal adults (nonallergic) were subjected into RT-PCR measuring the expression levels of *Duox2* (Fig. 7A). Interestingly, we found a significant increase in the *Duox2* gene expression level in sinusitis, compared to that in healthy adults. The result suggested that the upregulated expression of *Duox2* seems to be linked to infectious inflammatory diseases in the nasal mucosa. Moreover, our results are supported with the current study where exacerbation of chronic obstructive pulmonary disease is associated with overexpression of DUOX isozymes (40). Collectively, these results provide decisive evidence that oxidative stress is a critical factor in the development and progression of airway inflammation and DUOX2 plays a pivotal role in flagellin-induced inflammatory responses, including IL-8 production and MUC5AC expression in the airway epithelia.

Materials and Methods

Materials

NAC, allopurinol, dicumarol, and DPI were purchased from Sigma Aldrich. Purified flagellin, TLR5 antagonist (Anti-hTLR5-IgA), and its control antibody (control IgA1) were purchased from Invivogen. Unless otherwise stated, all other reagents were from Sigma.

Cell culture

After approval of the study protocol by the Institutional Review Board of the Yonsei University College of Medicine, human nasal middle turbinate specimens were obtained from healthy volunteers. The culture systems used for the NHNE cells have been described previously (23, 46). The air–liquid interface (ALI) was created on day 9 by removing the apical medium and feeding the cultures from only the basal compartment. The culture medium was changed daily after the ALI was initiated, and all experiments utilized NHNE cells 3 days after the creation of the ALI.

Mice

C57BL/6J (wild type) mice for the inhibitor experiment were purchased directly from Orient Bio, Inc. DUOX2 mutant mice were obtained from The Jackson Laboratory. The new, recessive *thyd* mutation arose spontaneously in a B6 (129)-*Duox2*^{thyd}/J mouse (Jackson Laboratory; Stock no. 005543). Molecular genotyping enabled direct identification of heterozygotes for simplified colony maintenance.

Methods

Quantitative RT-PCR

Quantitative RT-PCR was performed using TaqMan® universal PCR master mix. RT-PCR was performed using the PE Biosystems ABI PRISM® 7700 sequence detection system. Target-specific probe sets against *Duox1* or *Duox2* were purchased from Applied Biosystems. The relative quantity was obtained using the comparative threshold method and results were normalized against GAPDH as an endogenous control. Gene-specific primer and probe sets designed against the targeted molecules are listed in Supplementary Table S2.

Intracellular ROS assay by DCF-DA

ROS were measured by a method described previously (6). After the confluent cells were stimulated, they were washed with Hanks' balanced salt solution (HBSS) and incubated for 10 min in the dark at 37°Cin HBSS containing 10 μM DCF-DA (Molecular Probes). DCF fluorescence was measured using a Zeiss LSM 510 confocal microscope (Minneapolis, MN) at an excitation wavelength of 488 nm and an emission wavelength of 515–540 nm. Seven fields of each dish were randomly selected and the fluorescence intensity was measured with the Carl Zeiss vision system (KS400, version 3.0). The seven values were averaged to obtain the mean relative fluorescence intensity, and these means were used for comparisons. All experiments were repeated at least three times.

Preparation of recombinant FliC and mutant proteins

Salmonella enteritidis FliC flagellin gene (GenBank accession: No. M84980) was obtained by PCR. Wild-type FliC flagellin (AA 21-505) and deletion mutant form of FliC flagellin (AA 119-505) were cloned in the pMT/V5-His vector (Invitrogen) to generate C-terminal V5-His epitope-tagged recombinant protein. To secrete recombinant flagellin in the culture supernatant, the signal peptide of the *Drosophila* Spätzler gene (AA 1-22) was used by fusing directly to the wild-type or mutant FliC flagellin constructs. *Drosophila* Schneider cell line was used for the production of recombinant FliC. Transfection of these cells was conducted according to a standard protocol using $CaPO_4$. Expression of FliC flagellin was induced in cells by the addition of $CuSO_4$ to the culture medium at a final concentration of 500 μM for 48 h before harvesting. Recombinant proteins were purified from the culture supernatant by using Ni^+-NTA resin according to the manufacturer's instructions. The recombinant fliC protein was eluted from the resin with 250 mM of imidazole, and dialyzed with 50 mM sodium phosphate buffer (pH 7, 1% glycerol, 48 h).

Knockdown of Duox1 and Duox2 using lentiviruses

For knockdown of Duox1 and Duox2, cells were infected with control lentivirus, Duox1 (sc-60550-V) or Duox2 (sc-60552-V) shRNA lentivirus (Santa Cruz, CA), according to the manufacturer's protocol.

Preparation of antibodies against Duox1 and Duox2

Three peptides (41-53 EHRWGSKGSRLQR, 364-373 NSYWSREHP, and 451-461 QDINPALSRSN) for Duox1 and two peptides (370-381 CNNYWIRENPNL and 421-432 SRTDYVASSIQR) are synthesized from Peptron. Polyclonal

antibodies were generated from the injection of peptide mixture for Duox1 or Duox2 to rabbit (AbFrontier).

Preparation and analysis of NALF

Nasal passages were flushed with 0.5 ml of phosphate-buffered saline, of which an average of 0.45 ml was recovered into a 1.5 ml tube held to the nose of the mouse. Nasal wash fluid was centrifuged to remove cells and the supernatant was stored at −80°C until analysis. The cells collected from the NALF were counted in a hemacytometer. Two hundred microliters of cell suspension was dispersed onto slides using a cytospin machine set at 100 *g* for 5 min. Slides were stained using a Hemacolor stain set (Merck) according to the manufacturer's instructions.

Dot blot analysis for intracellular MUC5AC protein

MUC5AC protein was detected by a dot blot analysis as described previously (16). After treatment with flagellin, NHNE cells or mouse NALF were lysed with cell extraction buffer (Invitrogen) followed by sonication and centrifugation at 15,700 *g* for 10 min. Protein amounts were determined using the BCA protein assay (Pierce) and a dot blot analysis was performed.

Enzyme-linked immunosorbent assay of IL-8 secretion

The total level of IL-8 in cell culture supernatants was measured using a commercially available kit (R&D Systems) according to the manufacturer's instructions. Assays had a range of 10–2000 pg/mL.

Nonsurgical intranasal instillation for mice

Flagellin and other inhibitors were administered intranasally. For intranasal instillations, 25 μl of solution was applied drop-wise into each nostril.

Histology

The nasal tissue was prepared by removing the skin from the head before preserving in 10% formalin overnight, followed by decalcification for 5 h in Surgipath Decalcifier II solution. A coronal section immediately rostral to the eyes was embedded in paraffin, cut at 4 μm, and stained with hematoxylin and eosin by routine methods. For immunostaining, tissue sections were deparaffinized and rehydrated in graded alcohol. Nonspecific protein binding was blocked with 3% BSA and 2% goat serum in Tris-buffered saline (pH 8.0) with 0.2% Tween 20 (TBST) for 1 h. Primary antibodies were diluted in blocking buffer and incubated overnight at 4°C at a final concentration of 0.05 or 0.1 μg/ml for human and mouse tissue sections. For MUC5AC immunostaining, tissues were blocked with nonspecific background staining with blocking agent (Immunotech; 2391) and then incubated with mouse antibody to human MUC5AC (mouse monoclonal Ab 45M1, 2 μg/ml; Lab Vision Corp.). For neutrophil immunostaining, tissue sections were stained with the antibody (NIMP R14) Ly6g/Gr1 surface protein expressed in neutrophil (Abcam) or with control rat IgG, followed by detection with ABC-HRP kit and DAB substrate. Tissue sections were counterstained with hematoxylin, dehydrated in graded ethanol, and mounted for photomicrography.

Harvest of mouse nasal tissue

After euthanasia with a CO_2 gas chamber and cervical dislocation, the skin at the nape of the neck was incised with fine dissecting scissors, and the incision rotated around the entire neck (4). This skin was then dissected interiorly and completely removed, leaving the anterior aspect of the skull base exposed. The remaining portion of the skull was removed to the posterior aspect of the nasal cavity. The scissor was then turned inferiorly to section the palate, and thus completely separated the septum and turbinate from the lateral nasal wall. Once harvested, the nasal septum and turbinate's mucosa from each side was gently elevated off the cartilage and bone and total RNA was isolated from these tissues using TRIzol (Invitrogen).

Patient samples

Normal, healthy biopsies were derived from patients who had undergone septoplasty without pathological conditions. Sinusitis samples were taken from the patients with chronic sinusitis who did not have histories of asthma, aspirin sensitivity, or cystic fibrosis. None of the patients had received immunosuppressive drugs within the previous 2 weeks. They all had negative results on the allergic skin-prick test. All patient-related procedures were approved by the Yonsei University, Severance Hospital's ethics committee. All patients agreed to participate by giving informed consent at least 24 h before the study.

Accession numbers

Array data are deposited at the Gene Expression omnibus. Accession number is GSE26135.

Statistic analysis

Significant differences between treatment groups were identified with a *t*-test. *p*-Values less than 0.05 were considered statistically significant.

Additional details on methods are provided in an online Supplementary Methods.

Acknowledgments

We thank Drs. Kyu-Bo Kim and Karl-Heinz Krause for critical reading of the article. This research was supported by the Basic Science Research Program of the National Research Foundation of Korea (2011-0001168 to J.H.Y.), by the National Core Research Center (grant R15-2006-020-00000-0 to Y.S.B), by World Class University program (R31-2008-000-10010-0 to Y.S.B), by National Research Laboratory program (grant number ROA-2007-000-20004-00 to Y.S.B) of the Ministry of Education, Science and Technology/Korea Science and Engineering Foundation, and by Korea Health 21 R&D program grant A084614 of Ministry of Health and Welfare. M.S.S and J.O.K are recipients of a BK21 scholarship.

Author Disclosure Statement

No competing financial interests exist.

References

1. Adamo R, Sokol S, Soong G, Gomez MI, and Prince A. Pseudomonas aeruginosa flagella activate airway epithelial cells through asialoGM1 and toll-like receptor 2 as well as toll-like receptor 5. *Am J Respir Cell Mol Biol* 30: 627–634, 2004.

2. Ameziane-El-Hassani R, Morand S, Boucher JL, Frapart YM, Apostolou D, Agnandji D, Gnidehou S, Ohayon R, Noel-Hudson MS, Francon J, Lalaoui K, Virion A, and Dupuy C. Dual oxidase-2 has an intrinsic Ca2+-dependent H2O2-generating activity. *J Biol Chem* 280: 30046–30054, 2005.
3. Andersen-Nissen E, Smith KD, Strobe KL, Barrett SL, Cookson BT, Logan SM, and Aderem A. Evasion of Toll-like receptor 5 by flagellated bacteria. *Proc Natl Acad Sci U S A* 102: 9247–9252, 2005.
4. Antunes MB, Woodworth BA, Bhargave G, Xiong G, Aguilar JL, Ratner AJ, Kreindler JL, Rubenstein RC, and Cohen NA. Murine nasal septa for respiratory epithelial air-liquid interface cultures. *Biotechniques* 43: 195–196, 198, 200 passim, 2007.
5. Bae YS, Choi MK, and Lee WJ. Dual oxidase in mucosal immunity and host-microbe homeostasis. *Trends Immunol* 31: 278–287, 2010.
6. Bae YS, Kang SW, Seo MS, Baines IC, Tekle E, Chock PB, and Rhee SG. Epidermal growth factor (EGF)-induced generation of hydrogen peroxide. Role in EGF receptor-mediated tyrosine phosphorylation. *J Biol Chem* 272: 217–221, 1997.
7. Bae YS, Lee JH, Choi SH, Kim S, Almazan F, Witztum JL, and Miller YI. Macrophages generate reactive oxygen species in response to minimally oxidized low-density lipoprotein: toll-like receptor 4- and spleen tyrosine kinase-dependent activation of NADPH oxidase 2. *Circ Res* 104: 210–218, 21p following 218, 2009.
8. Bao L, Avshalumov MV, Patel JC, Lee CR, Miller EW, Chang CJ, and Rice ME. Mitochondria are the source of hydrogen peroxide for dynamic brain-cell signaling. *J Neurosci* 29: 9002–9010, 2009.
9. Boots AW, Hristova M, Kasahara DI, Haenen GR, Bast A, and van der Vliet A. ATP-mediated activation of the NADPH oxidase DUOX1 mediates airway epithelial responses to bacterial stimuli. *J Biol Chem* 284: 17858–17867, 2009.
10. De Deken X, Wang D, Many MC, Costagliola S, Libert F, Vassart G, Dumont JE, and Miot F. Cloning of two human thyroid cDNAs encoding new members of the NADPH oxidase family. *J Biol Chem* 275: 23227–23233, 2000.
11. Dohrman A, Miyata S, Gallup M, Li JD, Chapelin C, Coste A, Escudier E, Nadel J, and Basbaum C. Mucin gene (MUC 2 and MUC 5AC) upregulation by Gram-positive and Gram-negative bacteria. *Biochim Biophys Acta* 1406: 251–259, 1998.
12. Dupuy C, Ohayon R, Valent A, Noel-Hudson MS, Deme D, and Virion A. Purification of a novel flavoprotein involved in the thyroid NADPH oxidase. Cloning of the porcine and human cdnas. *J Biol Chem* 274: 37265–37269, 1999.
13. Fischer H. Mechanisms and function of DUOX in epithelia of the lung. *Antioxid Redox Signal* 11: 2453–2465, 2009.
14. Gattas MV, Forteza R, Fragoso MA, Fregien N, Salas P, Salathe M, and Conner GE. Oxidative epithelial host defense is regulated by infectious and inflammatory stimuli. *Free Radic Biol Med* 47: 1450–1458, 2009.
15. Gon Y. Toll-like receptors and airway inflammation. *Allergol Int* 57: 33–37, 2008.
16. Gray TE, Guzman K, Davis CW, Abdullah LH, and Nettesheim P. Mucociliary differentiation of serially passaged normal human tracheobronchial epithelial cells. *Am J Respir Cell Mol Biol* 14: 104–112, 1996.
17. Ha EM, Lee KA, Seo YY, Kim SH, Lim JH, Oh BH, Kim J, and Lee WJ. Coordination of multiple dual oxidase-regulatory pathways in responses to commensal and infectious microbes in drosophila gut. *Nat Immunol* 10: 949–957, 2009.
18. Hawn TR, Verbon A, Lettinga KD, Zhao LP, Li SS, Laws RJ, Skerrett SJ, Beutler B, Schroeder L, Nachman A, Ozinsky A, Smith KD, and Aderem A. A common dominant TLR5 stop codon polymorphism abolishes flagellin signaling and is associated with susceptibility to legionnaires' disease. *J Exp Med* 198: 1563–1572, 2003.
19. Hornsby MJ, Huff JL, Kays RJ, Canfield DR, Bevins CL, and Solnick JV. Helicobacter pylori induces an antimicrobial response in rhesus macaques in a cag pathogenicity island-dependent manner. *Gastroenterology* 134: 1049–1057, 2008.
20. Iwamura C, and Nakayama T. Toll-like receptors in the respiratory system: their roles in inflammation. *Curr Allergy Asthma Rep* 8: 7–13, 2008.
21. Johnson KR, Marden CC, Ward-Bailey P, Gagnon LH, Bronson RT, and Donahue LR. Congenital hypothyroidism, dwarfism, and hearing impairment caused by a missense mutation in the mouse dual oxidase 2 gene, Duox2. *Mol Endocrinol* 21: 1593–1602, 2007.
22. Kawai T, and Akira S. The role of pattern-recognition receptors in innate immunity: update on Toll-like receptors. *Nat Immunol* 11: 373–384, 2010.
23. Kim HJ, Park YD, Moon UY, Kim JH, Jeon JH, Lee JG, Bae YS, and Yoon JH. The role of Nox4 in oxidative stress-induced MUC5AC overexpression in human airway epithelial cells. *Am J Respir Cell Mol Biol* 39: 598–609, 2008.
24. Koff JL, Shao MX, Ueki IF, and Nadel JA. Multiple TLRs activate EGFR via a signaling cascade to produce innate immune responses in airway epithelium. *Am J Physiol Lung Cell Mol Physiol* 294: L1068–L1075, 2008.
25. Lambeth JD. NOX enzymes and the biology of reactive oxygen. *Nat Rev Immunol* 4: 181–189, 2004.
26. Lambeth JD, Kawahara T, and Diebold B. Regulation of Nox and Duox enzymatic activity and expression. *Free Radic Biol Med* 43: 319–331, 2007.
27. Mayer AK, and Dalpke AH. Regulation of local immunity by airway epithelial cells. *Arch Immunol Ther Exp (Warsz)* 55: 353–362, 2007.
28. McNamara N, Gallup M, Sucher A, Maltseva I, McKemy D, and Basbaum C. AsialoGM1 and TLR5 cooperate in flagellin-induced nucleotide signaling to activate Erk1/2. *Am J Respir Cell Mol Biol* 34: 653–660, 2006.
29. McNamara N, Khong A, McKemy D, Caterina M, Boyer J, Julius D, and Basbaum C. ATP transduces signals from ASGM1, a glycolipid that functions as a bacterial receptor. *Proc Natl Acad Sci U S A* 98: 9086–9091, 2001.
30. Medzhitov R. Toll-like receptors and innate immunity. *Nat Rev Immunol* 1: 135–145, 2001.
31. Moreno JC, Bikker H, Kempers MJ, van Trotsenburg AS, Baas F, de Vijlder JJ, Vulsma T, and Ris-Stalpers C. Inactivating mutations in the gene for thyroid oxidase 2 (THOX2) and congenital hypothyroidism. *N Engl J Med* 347: 95–102, 2002.
32. Ogier-Denis E, Mkaddem SB, and Vandewalle A. NOX enzymes and Toll-like receptor signaling. *Semin Immunopathol* 30: 291–300, 2008.
33. Park HS, Jung HY, Park EY, Kim J, Lee WJ, and Bae YS. Cutting edge: direct interaction of TLR4 with NAD(P)H oxidase 4 isozyme is essential for lipopolysaccharide-induced production of reactive oxygen species and activation of NF-kappa B. *J Immunol* 173: 3589–3593, 2004.

34. Prince A. Flagellar activation of epithelial signaling. *Am J Respir Cell Mol Biol* 34: 548–551, 2006.
35. Rada B, and Leto TL. Oxidative innate immune defenses by Nox/Duox family NADPH oxidases. *Contrib Microbiol* 15: 164–187, 2008.
36. Raoust E, Balloy V, Garcia-Verdugo I, Touqui L, Ramphal R, and Chignard M. Pseudomonas aeruginosa LPS or flagellin are sufficient to activate TLR-dependent signaling in murine alveolar macrophages and airway epithelial cells. *PLoS One* 4: e7259, 2009.
37. Raz E. Organ-specific regulation of innate immunity. *Nat Immunol* 8: 3–4, 2007.
38. Reichhart JM. TLR5 takes aim at bacterial propeller. *Nat Immunol* 4: 1159–1160, 2003.
39. Rigutto S, Hoste C, Grasberger H, Milenkovic M, Communi D, Dumont JE, Corvilain B, Miot F, and De Deken X. Activation of dual oxidases Duox1 and Duox2: differential regulation mediated by camp-dependent protein kinase and protein kinase C-dependent phosphorylation. *J Biol Chem* 284: 6725–6734, 2009.
40. Schneider D, Ganesan S, Comstock AT, Meldrum CA, Mahidhara R, Goldsmith AM, Curtis JL, Martinez FJ, Hershenson MB, and Sajjan U. Increased Cytokine Response of Rhinovirus-infected Airway Epithelial Cells in Chronic Obstructive Pulmonary Disease. *Am J Respir Crit Care Med* 182: 332–340, 2010.
41. Shao MX, and Nadel JA. Dual oxidase 1-dependent MUC5AC mucin expression in cultured human airway epithelial cells. *Proc Natl Acad Sci U S A* 102: 767–772, 2005.
42. Smith KD, Andersen-Nissen E, Hayashi F, Strobe K, Bergman MA, Barrett SL, Cookson BT, and Aderem A. Toll-like receptor 5 recognizes a conserved site on flagellin required for protofilament formation and bacterial motility. *Nat Immunol* 4: 1247–1253, 2003.
43. van der Vliet A. NADPH oxidases in lung biology and pathology: host defense enzymes, and more. *Free Radic Biol Med* 44: 938–955, 2008.
44. Vignais PV. The superoxide-generating NADPH oxidase: structural aspects and activation mechanism. *Cell Mol Life Sci* 59: 1428–1459, 2002.
45. Wesley UV, Bove PF, Hristova M, McCarthy S, and van der Vliet A. Airway epithelial cell migration and wound repair by ATP-mediated activation of dual oxidase 1. *J Biol Chem* 282: 3213–3220, 2007.
46. Yoon JH, Gray T, Guzman K, Koo JS, and Nettesheim P. Regulation of the secretory phenotype of human airway epithelium by retinoic acid, triiodothyronine, and extracellular matrix. *Am J Respir Cell Mol Biol* 16: 724–731, 1997.

Address correspondence to:
Dr. Yun Soo Bae
Department of Life Science
Ewha Womans University
Seoul 120-750
Korea

E-mail: baeys@ewha.ac.kr

Dr. Joo-Heon Yoon
Department of Otorhinolaryngology
Yonsei University College of Medicine
134 Shinchon-dong, Seodaemun-gu
Seoul 120-752
Korea

E-mail: jhyoon@yuhs.ac

Date of first submission to ARS Central, January 19, 2011; date of final revised submission, June 29, 2011; date of acceptance, June 29, 2011.

Abbreviations Used

ALI = air–liquid interface
BAPTA-AM = 1,2-Bis(2-aminophenoxy)ethane-N,N,N′,N′-tetraacetic acid
DCF-DA = 2′,7′-dichlorofluorescin diacetate
DMSO = dimethyl sulfoxide
DPI = diphenyleneiodonium sulfate
DUOX = dual oxidase
EF = helix-loop-helix structural domain
EGTA = ethylene glycol tetraacetic acid
ELISA = enzyme-linked immunosorbent assay
H_2O_2 = hydrogen peroxide
HBSS = Hanks' balanced salt solution
i.n. = intranasal
IP = immunoprecipitation
NAC = *N*-acetyl-L-cysteine
NALF = nasal lavage fluid
NF-κB = nuclear factor kappa B
NHNE = normal human nasal epithelial cells
NOX = NADPH oxidase
PBS = phosphate-buffered saline
PK = protein kinase
ROS = reactive oxygen species
RT-PCR = real-time polymerase chain reaction
SDS-PAGE = sodium dodecyl sulfate–polyacrylamide gel electrophoresis
TIR = toll/interleukin-1β receptor
TLR = toll-like receptors

This article has been cited by:

1. Ji-Hwan Ryu, Jung-Yeon Yoo, Min-Ji Kim, Sang-Gyu Hwang, Kwang Chul Ahn, Jae-Chan Ryu, Mi-Kyung Choi, Jung Hee Joo, Chang-Hoon Kim, Sang-Nam Lee, Won-Jae Lee, Jaesang Kim, Dong Min Shin, Mi-Na Kweon, Yun Soo Bae, Joo-Heon Yoon. 2012. Distinct TLR-mediated pathways regulate house dust mite–induced allergic disease in the upper and lower airways. *Journal of Allergy and Clinical Immunology* . [CrossRef]